

Disk-jet connection in Cygnus X-3

M. Choudhury¹, A. R. Rao¹, S. V. Vadawale¹, C. H. Ishwara-Chandra², and A. K. Jain²

¹ Tata Institute of Fundamental Research, Mumbai 400005, India

² ISRO Satellite Center, Bangalore 560017, India

Received 19 November 2001 / Accepted 16 January 2002

Abstract. We present the results of a detailed correlation study between the soft X-ray, hard X-ray, and radio emission (obtained from *RXTE ASM*, *BATSE*, and GBI observations, respectively) of the bright radio emitting Galactic X-ray binary Cygnus X-3. We detect a very strong positive correlation between the soft X-ray and radio emission during the low-hard and minor flaring periods of the source, and an anti-correlation between the soft and hard X-ray emissions. We present statistical arguments to suggest that the anti-correlation between the radio and hard X-ray emission, reported earlier, is primarily due to their correlation and anti-correlation, respectively, with the soft X-ray emission. We make a wide band X-ray spectral study using the pointed *RXTE* observations and detect a pivotal behaviour in the X-ray spectrum. We argue that this X-ray spectral pivoting is responsible for the anti-correlation between the soft and hard X-ray emissions. The strong correlation between the soft X-ray and radio emission suggests a close link between the accreting mechanism, plasma cloud surrounding the compact object and the radio emission.

Key words. accretion – binaries: close – stars: individual: Cygnus X-3 – radio continuum: stars – X-rays: binaries

1. Introduction

Cygnus X-3 is the brightest radio source ever associated with an X-ray binary, in both quiescent and flare states (Waltman et al. 1995). It is located at a distance of 9 kpc (Predehl et al. 2000) in the Galactic plane in one of the arms. It exhibits multiple radio outbursts correlated with the high-soft state in the X-ray emission (Watanabe et al. 1994). The VLBI observations of one such major flare revealed a core jet (Mioduszewski et al. 2001), although it is not unambiguously resolved whether the jet is one-sided or two-sided (Marti et al. 2001). Watanabe et al. (1994) also hint at a correlation between the soft X-ray (as observed by ASM aboard the Ginga observatory) and the quiescent radio emission (as seen by the GBI), during the low-hard state. McCollough et al. (1999) give a detailed correlation test between the hard X-ray (as observed by the BATSE aboard the CGRO) and the radio (GBI), in the various states of radio and X-ray emission. They report 1) anti-correlation between the radio and hard X-ray emission during the quiescent period, 2) correlation between the radio and hard X-ray emission during the major flaring period, and 3) no correlation between the radio and hard X-ray emission during the minor flaring period.

The (quasi) simultaneous observations of X-ray binaries in the radio and X-ray bands has led to the notion that the presence of radio jets is *ubiquitous* in sources

with black holes or low magnetic field ($\leq 10^9$ G) neutron stars as compact objects and these sources show a definite connection between the accretion (inflow) mechanism and the jet (outflow) formation (see Fender et al. 2001). Correlation between radio and soft X-ray emission has been established for at least two Galactic blackhole candidates (BHCs), Cygnus X-1 (Brocksopp et al. 1999) and GX 339-4 (Corbel et al. 2000). In this *Letter* we report the detection of a very strong correlation between the soft X-ray (as seen by the ASM aboard the *RXTE*) and the radio (GBI) during the low-hard and minor flaring state of Cygnus X-3, along with an anti-correlation between the hard X-ray (BATSE) and both soft X-ray (ASM) and radio (GBI) emissions. The soft X-ray: radio correlation is definitely stronger and more significant than the anti-correlation between the hard X-ray and the soft X-ray (and radio). We also carry out a detailed wide band spectral analysis, with available pointed *RXTE* observations during the low-hard state.

2. Data and analysis

The daily monitoring data are obtained from the archives of the respective observatories: soft X-ray, in the energy range 2–10 keV, from ASM (aboard *RXTE*), hard X-ray in the energy range 20–600 keV from BATSE (aboard CGRO) and radio at 2.2 and 8.3 GHz from GBI (Green Bank Interferometer, at Green Bank site, West Virginia, operated by NRAO). The pointed observations of both the narrow field of view instruments aboard the *RXTE*,

Send offprint requests to: M. Choudhury,
e-mail: manojulu@tifr.res.in

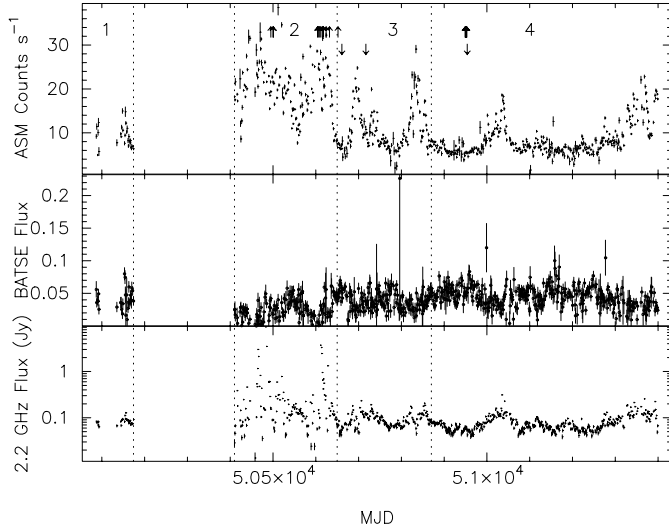


Fig. 1. The combined simultaneous lightcurve of Cygnus X-3 in the soft X-ray (ASM, top panel), hard X-ray (BATSE, middle panel) and the radio (GBI, bottom panel). The various “states” of the source are separated by vertical dashed lines and identified with numbers. The arrows on the top panel give the start time of RXTE pointed observations and the three inverted arrows give the days for which wideband X-ray spectral studies are carried out.

viz. PCA and HEXTE, are analysed for wide-band spectral study by combining the data from both, which include 129 channel PHA data from PCA standard-2 data (all PCUs added) and 64 channel data from the Cluster-0 of HEXTE. After analysing data from the Crab nebula, Vadawale et al. (2001) suggest using only Cluster-0 data from HEXTE and adding a systematic error of 2% to PCA data for a proper fit, and we have followed the same recipe. The basic data reduction and analysis was carried out using FTOOLS (V5.0) and XSPEC (V11.0).

In Fig. 1 we plot the daily averaged lightcurve of Cygnus X-3 as seen by ASM (top panel), BATSE (middle panel) and GBI (2.2 GHz, bottom panel), during the period when all these three detectors were simultaneously monitoring the source. Historically, the behaviour of radio emission in Cygnus X-3 is classified into: 1) quiescent period (~ 50 – 100 mJy), 2) major flaring (≥ 1 Jy) with a preceding quenched state (~ 10 – 20 mJy), and 3) minor flaring (≥ 100 – 150 mJy) with partial quenching state (see Waltman et al. 1995; McCollough et al. 1999). Accordingly we have demarcated four regions in Fig. 1, region 1 and 4 corresponding to the quiescent state (although region 4 contains two minor flares along with the long quiescent period), region 2 corresponding to the major flaring state and region 3 corresponding to the minor flaring state.

To test for the correlation among the soft X-ray, hard X-ray and the radio emission we have used the Spearman Rank Correlation (SRC) coefficient adapting the method prescribed by Macklin (1982) and have derived the corresponding D -parameter, which gives the confidence level, in terms of standard deviations, that the derived correlation is not due to the influence of the third parameter.

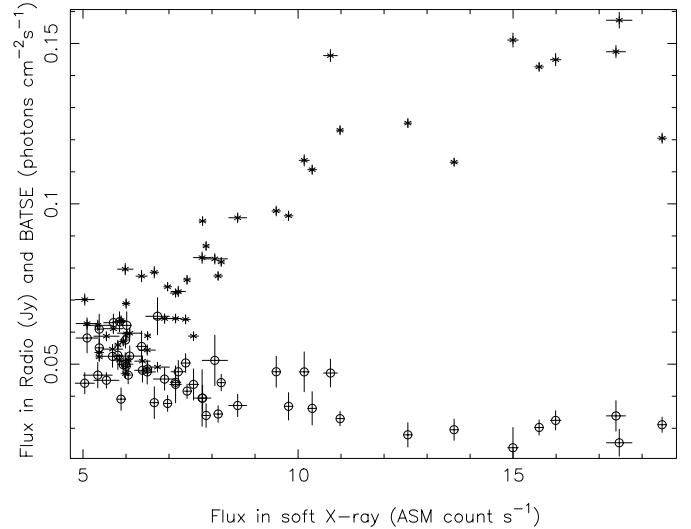


Fig. 2. The variation of flux in radio (GBI, 2.2 GHz, shown as plus signs) and hard X-ray (BATSE, 20–600 keV, shown as circles) with soft X-ray (ASM, 2–10 keV), during the low-hard state of Cygnus X-3 (region 4 of Fig. 1). Each data point is an average value for 10 days.

Table 1 shows the SRC coefficient, null hypothesis probability and the D -parameter, using 10 day averages of the data for the different periods (and their combination) as demarcated in Fig. 1. Reducing the number of days for averaging does not significantly change the results. The number of data points in region 1 (of Fig. 1) is meagre and hence is not included in the correlation tests.

The most interesting result is that the soft X-ray and radio are very strongly correlated, with a very high significance level, in region 4 and regions 3 & 4 combined. It can also be ruled out (at $>5\sigma$ level) that this correlation is influenced by the third parameter, the hard X-ray emission. Though these two parameters are correlated even in the flaring state (region 2) at a much reduced significance level, the correlation tests in this region could be influenced by the high variability at time scales shorter than the period chosen for taking the averages (10 days). Hence we concentrate on the results obtained for region 4 and region 3 & 4 combined. It is also found that the soft X-ray is anti-correlated with the hard X-ray emission. The anti-correlation between the radio and hard X-ray emission, though strong, could be influenced by the other two correlations, particularly when we examine the data for the region 3 & 4 combined. The similarity of the behaviour of region 4 and regions 3 & 4 combined suggest that the emission mechanism during the minor flaring and the quiescent period are the same, and hence these two can be clubbed together as one class.

Figure 2, showing the variation of flux in radio (correlated) and hard X-ray (anti-correlated) with soft X-ray flux during the low-hard state (region 4 of Fig. 1), clearly demonstrates the simple monotonic dependence of the both with the soft X-ray (ASM) during the few hundred days. A total of 22 pointed observations of RXTE, of which

Table 1. The Spearman Rank Correlation (SRC) coefficient, null-hypothesis probability and D-parameter between the radio, soft X-ray and hard X-ray for different periods demarcated in Fig. 1.

	SRC coeff.	Null Prob.	D-Parameter
Region 4			
ASM:GBI	0.84	6.3×10^{-11}	5.2
GBI:BATSE	-0.75	9.2×10^{-11}	-2.7
ASM:BATSE	-0.74	3.1×10^{-11}	-2.2
Region 3			
ASM:GBI	0.66	8.3×10^{-4}	2.7
GBI:BATSE	-0.43	4.7×10^{-2}	0.4
ASM:BATSE	-0.71	1.9×10^{-4}	-3.2
Region 2			
ASM:GBI	0.56	3.5×10^{-3}	4.1
GBI:BATSE	0.10	6.3×10^{-1}	2.7
ASM:BATSE	-0.50	1.1×10^{-2}	-3.8
Region 3 & 4			
ASM:GBI	0.83	2.1×10^{-20}	6.2
GBI:BATSE	-0.72	4.7×10^{-13}	-1.5
ASM:BATSE	-0.79	4.1×10^{-17}	-3.8

Table 2. The observed flux and X-ray spectral parameters of Cygnus X-3 during the three pointed RXTE observations.

	MJD		
	50717	50661	50954
A. Flux			
ASM (cts s^{-1})	11.11	8.18	5.37
BATSE ($\text{ph cm}^{-2}\text{s}^{-1}$)	0.038	0.051	0.058
GBI-2.2 GHz (mJy)	115	64	43
GBI-8.3 GHz (mJy)	165	73	53
B. Best fit parameters for CompST+power law			
kT_e (keV)	5.09 ± 0.38	4.37 ± 0.04	4.87 ± 0.08
Γ_x	2.55 ± 0.22	2.19 ± 0.05	2.01 ± 0.04
χ^2_{ν} (d.o.f.)	0.74(86)	1.80(59)	1.42(108)

10 are in the low-hard state, exist during this period of simultaneous monitoring (shown in the top panel of Fig. 1). Only three groups of observations, separated by more than ten days, exist, in the low-hard state. We have selected representative observation from each group, marked as inverted arrows in Fig. 1, for a detailed X-ray spectral analysis. These three observations span the range of observed X-ray and radio fluxes and some salient features of these observations are given in Table 2. The three unfolded spectra are overlaid on the top panel of Fig. 3 with the PHA ratios for the two extreme spectra shown in the bottom panel.

During the low-hard state, encompassing the regions 3 & 4 of Fig. 1, the continuum spectra (5–150 keV) is best described by the Comptonization of seed photons from a thermal multi-coloured accretion disk by a thermal Comptonizing plasma cloud (CompST-Sunyaev & Titarchuk 1980; Nakamura et al. 1993; Rajeev et al. 1994) along with a non-thermal powerlaw emission (Choudhury & Rao 2001). The resolution of the three Fe lines

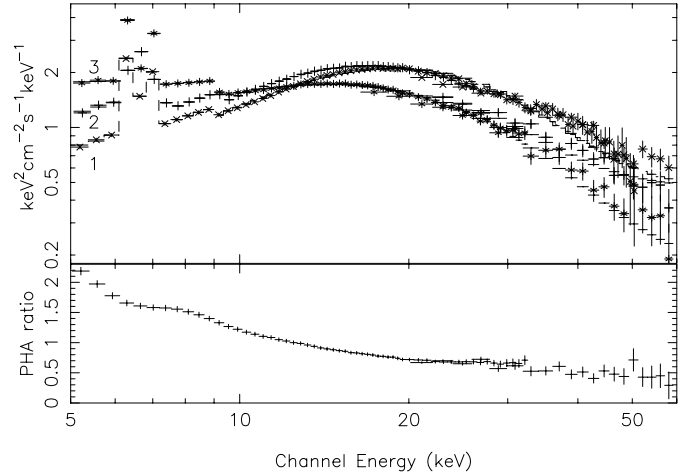


Fig. 3. Top panel: the unfolded X-ray spectra of Cygnus X-3 during the radio quiescent period on three different occasions (1: MJD 50954; 2: MJD 50661; 3: MJD 50717). Bottom panel: PHA ratio of spectra from the extreme observations.

(Kitamoto et al. 1994) and the two absorption edges (Rajeev et al. 1994) are beyond the capability of the PCA, hence we fix the relative separation of line and edge energies as reported by Rajeev et al. (1994); Nakamura et al. (1993); and Kitamoto et al. (1994), and treat the edge energy at 7.1 keV and the normalization of all the lines and edges as the variable parameters in the fit. The best fit values of the electron temperature (kT_e) of the Compton cloud and the powerlaw photon index (Γ_x) for the three spectra are given in Table 2B. Other simple models like cutoff powerlaw (along with a powerlaw), broken powerlaw, etc. do not consistently fit all the observed spectra with physically feasible parameter values and give much inferior fits. It can be seen from the figure that there is a systematic change in the shape of the spectrum with increasing soft X-ray flux (and radio flux, see Table 2). The X-ray spectrum, when the radio flux is low, is quite flat in the 20–40 keV region and the spectral curvature increases with the soft X-ray flux.

3. Discussion and conclusion

Although Galactic BHCs exhibit radio jets during the low-hard state, viz. Cygnus X-1 (Brocksopp et al. 1999), GX 339-4 (Corbel et al. 2000), GRS 1915+105 (Dhawan et al. 2000), XTE J1550-534 (Corbel et al. 2001), 1E 1740.7 (Mirabel et al. 1992), GRS 1758-258 (Rodriguez et al. 1992), a detailed correlation among the radio, soft and hard X-ray emission is done for a very few sources, viz. Cygnus X-1 and GX 339-4, and their behaviour is quite different from that of Cygnus X-3. Cygnus X-3 is the only source that shows such a strong correlation between soft X-ray and radio, and it is also the only source to distinctly show the anti-correlation between the soft and hard X-rays, during the low-hard state. Watanabe et al. (1994) have examined the association of the X-ray (from Ginga) and radio emission from Cygnus X-3 and though

there was a hint of correlation between the soft X-ray and radio flux in the hard state (see their Fig. 6), a detailed correlation was not presented, presumably because of the sparse sampling of the source by the Ginga satellite.

The quiescent state of Cygnus X-3 has persistent (flat spectrum) radio emission (60–100 mJy). This state in Cygnus X-3 is likely to be similar to the “plateau” radio state seen in the most active micro-quasar GRS 1915+105 which shows flat spectrum radio emission for extended durations and the radio emission is identified with a compact jet of size ~ 10 AU (Dhawan et al. 2000). The spectral changes in association with the radio emission is also quite similar to GRS 1915+105 (Vadawale et al. 2001).

Recently it has been suggested that X-ray emission from BHCs GRS 1915+105 (particularly during the “plateau” state) and XTE J1118+480 could be arising from synchrotron emission from the base of the jet (Vadawale et al. 2001; Markoff et al. 2001). Therefore it leads to a speculation that some of the X-ray flux in Cygnus X-3 also could be arising from synchrotron emission from the base of the jet. This can explain the correlation between soft X-ray and radio fluxes but fails to explain the anti-correlation between soft and hard X-ray fluxes.

It is also possible that the soft X-ray emission is due to the accretion disk (directly or indirectly) and the observed correlation is due to a connection between the accretion disk and the jet emission. The X-ray emission from Cygnus X-3 is highly obscured and the bulk of the X-ray emission below 5 keV is due to the emission-line dominated photo-ionized plasma surrounding the compact object (Paerels et al. 2000; Kawashima & Kitamoto 1996). Hence there is no clear evidence for the disk blackbody emission, commonly seen as an X-ray spectral component in the soft X-ray region in other BHCs. Our spectral analysis above 5 keV has identified two spectral components and these, by analogy with other BHCs, can be identified with thermal/non-thermal Comptonization (Zdziarski et al. 2001; Gierlinski et al. 1999) occurring in the source (or due to X-ray synchrotron emission – see above). If we assume that the region of the Comptonization is confined to a small region near the compact object, we can qualitatively explain the observed correlations under the Two Component Accretion Flow (TCAF) model of Chakrabarti (1996), in which the Compton spectrum originates from a region close to the compact object, confined within the Centrifugal Boundary Layer (CENBOL). At low accretion rate, the CENBOL is far away from the compact object, the spectrum is harder with lower outflow (see Das & Chakrabarti 1999). On increasing the accretion rate the CENBOL comes closer to the compact object with greater outflow, giving rise to increased radio emission. Though this model qualitatively explains the observed correlations, we must add here that the thermal Compton model is only an approximation and a correct Comptonization model requires an accurate description of the geometry of the emission region.

Acknowledgements. This research has made use of data obtained through the HEASARC Online Service, provided by the NASA/GSFC, and the Green Bank Interferometer, a facility of the National Science Foundation operated by the NRAO in support of NASA High Energy Astrophysics Programs. We thank J. S. Yadav for useful suggestions and H. Falcke, the referee of the paper, whose critical comments helped in significantly improving the quality of the work. AKJ is grateful to P. S. Goel, Director, ISAC and K. Kasturirangan, Chairman, ISRO, for their constant encouragement and support during the course of this work.

References

- Brocksopp, C., Fender, R. P., Larionov, V., et al. 1999, *MNRAS*, 309, 1063
- Chakrabarti, S. K. 1996, *Phys. Rep.*, 266, 229
- Choudhury, M., & Rao, A. R. 2001, to appear in the proceedings of International conference on Multicolour Universe at TIFR, Mumbai, India, 11–14 Sep., 2001
- Corbel, S., Fender, R. P., Tzioumis, A. K., et al. 2000, *A&A*, 359, 251
- Corbel, S., Kaaret, P., Jain, R. K., et al. 2001, *ApJ*, 554, 43
- Das, T., & Chakrabarti, S. K. 1999, *Class. & Quant. Gravity*, 16, 3879
- Dhawan, V., Mirabel, I. F., & Rodriguez, L. F. 2000, *ApJ*, 543, 373
- Fender, R. P. 2001 [[astro-ph/0109502](#)]
- Gierlinski, M., Zdziarski, A. A., Poutanen, J., et al. 1999, *MNRAS*, 309, 496
- Kawashima, K., & Kitamoto, S. 1996, *PASJ*, 48, L113
- Kitamoto, S., Kawashima, K., Negoro, H., et al. 1994, *PASJ*, 46, L105
- Macklin, J. T. 1982, *MNRAS*, 199, 1119
- Markoff, S., Falcke, H., & Fender, R. 2001, *A&A*, 372, L25
- Marti, J., Paredes, J. M., & Peracaula, M. 2001, *A&A*, 375, 476
- McCullough, M. L., Robinson, C. R., Zhang, S. N., et al. 1999, *ApJ*, 517, 951
- Mioduszewski, A. J., Rupen, M. P., Hjellming, R. J., et al. 2001, *ApJ*, 553, 766
- Mirabel, I. F., Rodriguez, L. F., Cordier, B., et al. 1992, *Nature*, 358, 215
- Nakamura, H., Matsuoka, M., Kawai, N., et al. 1993, *MNRAS*, 261, 353
- Paerels, F., Cottam, J., Sako, M., et al. 2000, *ApJ*, 533, L135
- Predehl, P., Burwitz, V., Paerels, F., et al. 2000, *A&A*, 357, L25
- Rajeev, M. R., Chitnis, V. R., Rao, A. R., et al. 1994, *ApJ*, 424, 376
- Rodriguez, L. F., Mirabel, I. F., & Marti, J. 1992, *ApJ*, 401, L15
- Sunyaev, R. A., & Titarchuk, L. G. 1980, *A&A*, 86, 121
- Vadawale, S. V., Rao, A. R., Nandi, A., et al. 2001, *A&A*, 370, L17
- Waltman, E. B., Ghigo, F. D., Johnston, K. J., et al. 1995, *AJ*, 110, 290
- Watanabe, H., Kitamoto, S., Miyamoto, S., et al. 1994, *ApJ*, 433, 350
- Zdziarski, A. A., Grove, E., Poutanen, J., et al. 2001, *ApJ*, 554, L45